Nihei Y, Ito D, Okada Y, Akamatsu W, Yagi T, Yoshizaki T, Okano H, Suzuki N.	Enhanced aggregation of androgen receptor in induced pluripotent stem cell-derived neurons from spinal and bulbar muscular atrophy.	J Biol Chem.		Epub ahead of print	2013
Veraitch O, Kobayashi T, Imaizumi Y, Akamatsu W, Sasaki T, Yamanaka , Amagai M, Okano H and Ohyama	Human induced pluripotent stem cell-derived ectodermal precursor cells contribute to hair follicle morphogenesis in vivo.	J Invest Dermatol.			2013
Imaizumi Y, Okada Y, Akamatsu W, Koike M, Kuzumaki N, Hayakawa H, Nihira T, Kobayashi T, Ohyama M, Sato S, Takanashi M, Funayama M, Hirayama A, Soga T, Hishiki T, Suematsu M, Yagi T, Ito D, Kosakai A, Hayashi K, Shouji M, Nakanishi A, Suzuki N, Mizuno Y, Mizushima N, Amagai M, Uchiyama Y, Mochizuki H, Hattori N, Okano H.	Mitochondrial dysfunction associated with increased oxidative stress and alpha-synuclein accumulation in PARK2 iPSC-derived neurons and postmortem brain tissue.	Mol Brain.	5(1)	35	2012
Matsui T, Akamatsu W, Nakamura M, Okano H.	Regeneration of the damaged central nervous system through reprogramming technology: basic concepts and potential application for cell replacement therapy.	Exp Neurol.	S0014 -4886 (12)	00378-0	2012
Imamura M, Okuno H, Tomioka I, Kawamura Y, Lin ZY, Nakajima R, Akamatsu W, Okano HJ, Matsuzaki Y, Sasaki E, Okano H.	Derivation of induced pluripotent stem cells by retroviral gene transduction in Mammalian species.	Methods Mol Biol.	925	21-48	2012
Yagi T, Kosakai A, Ito D, Okada Y, Akamatsu W, Nihei Y, Nabetani A, Ishikawa F, Arai Y, Hirose N, Okano H, Suzuki N.	Establishment of induced pluripotent stem cells from centenarians for neurodegenerative disease research.	PLoS ONE	7(7)	e41572	2012
Matsui T, Takano M, Yoshida K, Ono S, Fujisaki C, Matsuzaki Y, Yoshiaki Toyama Y, Nakamura M, Okano H, Akamatsu W.	Neural stem cells directly differentiated from partially reprogrammed fibroblasts rapidly acquire gliogenic competency.	Stem Cells	30(6)	1109-1119	2012

Matsui H, Sato F, Sato S, Koike M, Taruno Y, Saiki S, Funayama M, Ito H, Taniguchi Y, Uemura N, Toyoda A, Sakaki Y, Takeda S, Uchiyama Y, Hattori N, Takahashi R.	ATP13A2 Deficiency Induces a Decrease in Cathepsin D Activity, Fingerprint-like Inclusion Body Formation, and Selective Degeneration of Dopaminergic Neurons.	FEBS Lett		In press	2013
Matsui H, Gavinio R, Asano T, Uemura N, Ito H, Taniguchi Y, Kobayashi Y, Maki T, Shen J, Takeda S, Uemura K, Yamakado H, Takahashi R.	PINK1 and Parkin complementarily protect dopaminergic neurons in vertebrates.	Hum Mol Genet		In press	2013
Ishikawa T, Okada T, Ishikawa-Fujiwara T, Todo T, Kamei Y, Shigenobu S, Tanaka M, Saito TL, Yoshimura J, Morishita S, Toyoda A, Sakaki Y, Taniguchi Y, Takeda S, Mori K.	ATF6α/β-mediated Adjustment of ER Chaperone Levels Is Essential for Development of the Notochord in Medaka Fish.	Mol Biol Cell		In press	2013
Morita A, Nakahira K, Hasegawa T, Uchida K, Taniguchi Y, Takeda S, Toyoda A, Sakaki Y, Shimada A, Takeda H, Yanagihara I	Establishment and characterization of Roberts syndrome and SC phocomelia model medaka (Oryzias latipes).	Dev Growth Differ.	54	588-604	2012
Isoe Y, Okuyama T, Taniguchi Y, Kubo T, Takeuchi H.	p53 Mutation suppresses adult neurogenesis in medaka fish (Oryzias latipes).	Biochem Biophys Res Commun.	423	627-631	2012
Nakamura S, Watakabe I, Nishimura T, Picard JY, Toyoda A, Taniguchi Y, di Clemente N, Tanaka M.	Hyperproliferation of mitotically active germ cells due to defective anti-Müllerian hormone signaling mediates sex reversal in medaka.	Development	139	2283-2287	2012
Nakamura S, Watakabe I, Nishimura T, Toyoda A, Taniguchi Y, Tanaka M.	Analysis of medaka sox9 orthologue reveals a conserved role in germ cell maintenance.	PLoS One.	7	e29982	2012
Ishikawa T, Taniguchi Y, Okada T, Takeda S, Mori K.	Vertebrate unfolded protein response: mammalian signaling pathways are conserved in Medaka fish.	Cell Struct Funct.	36	247-259	2011

〔V〕

研究成果の刊行物・別冊

Acta Oto-Laryngologica, 2012; 132: 1160–1167

informa
healthcare

ORIGINAL ARTICLE

Unilateral cochlear nerve hypoplasia in children with mild to moderate hearing loss

HIDENOBU TAIJI[1], NORIKO MORIMOTO[1] & TATSUO MATSUNAGA[2]

[1]*Department of Otorhinolaryngology, National Center for Child Health and Development and* [2]*Laboratory of Auditory Disorders, National Institute of Sensory Organs, National Tokyo Medical Center, Tokyo, Japan*

Abstract

Conclusion: Even if hearing loss is mild to moderate, the presence of cochlear nerve (CN) hypoplasia associated with retrocochlear disorders should be considered. *Objectives:* CN hypoplasia is a term that refers to an absent cochlear nerve on high-resolution magnetic resonance imaging (MRI). Most cases of CN hypoplasia are associated with profound hearing loss. The present study reports six pediatric cases of unilateral CN hypoplasia with mild to moderate hearing loss. *Methods:* Between May 2008 and April 2011, pure-tone hearing tests were performed in 17 patients who were diagnosed with CN hypoplasia on high resolution for evaluation of unilateral sensorineural hearing loss at the National Center for Child Health and Development. Of these, six patients had average hearing levels in the affected ears of < 60 dB and were therefore included in this study. *Results:* All six ears with CN hypoplasia were associated with CN canal stenosis. DPOAEs were present in one (17%) of the six affected ears. The ABR thresholds of the ears with CN hypoplasia were significantly elevated compared with 1–4 kHz pure-tone hearing levels in one of three cases. In two of five cases, the maximum word recognition scores of the affected ears were poor compared with pure-tone hearing levels.

Keywords: *3-D constructive interference, steady-state magnetic resonance imaging, word recognition score, sensorineural hearing loss*

Introduction

Cochlear nerve (CN) hypoplasia refers to the absence of a visible CN on oblique sagittal magnetic resonance (MR) images of the lateral aspect of the inner auditory canal (IAC). CN hypoplasia is not an uncommon cause of congenital hearing loss as previously thought [1,2]. Although it is believed that most cases of CN hypoplasia are associated with profound hearing loss [1], a recent report presented a case of CN hypoplasia with moderate hearing loss limited to high frequencies [3]. The present study reports six pediatric cases of unilateral CN hypoplasia with mild to moderate hearing loss, and demonstrates that retrocochlear hearing loss is the predominant audiologic characteristic in these children.

Material and methods

Patient population

Between May 2008 and April 2011, 25 children who presented for evaluation of unilateral sensorineural hearing loss (SNHL) at the National Center for Child Health and Development were diagnosed with CN hypoplasia on high-resolution MR imaging (MRI).

Pure-tone hearing tests could be performed in 17 of these 25 children. Pure-tone audiometry was evaluated based on the three-tone average formulated by (a+b+c)/3, where a, b, and c are hearing levels at 0.5, 1, and 2 kHz, respectively. Eleven cases had profound hearing loss in the affected ears, with average hearing levels of >90 dB. The average hearing levels

Correspondence: Hidenobu Taiji MD, Department of Otorhinolaryngology, National Center for Child Health and Development, 2-10-1 Okura, Setagaya-ku, Tokyo 157-8535, Japan. Tel: +81 3 3416 0181. Fax: +81 3 5494 7909. E-mail: taijih5@gmail.com

(Received 20 April 2012; accepted 12 May 2012)

ISSN 0001-6489 print/ISSN 1651-2251 online
DOI: 10.3109/00016489.2012.696781

Table I. Audiologic and radiologic findings in children with unilateral cochlear nerve (CN) hypoplasia.

Case no.	Age (years)/sex	Side	Audiologic findings in affected ear: Pure-tone hearing level (dB)	ABR thresholds (dB nHL)	Maximum speech discrimination (%)	DPOAE	CNC diameter (mm): Affected ear	Healthy ear
1	6/F	R	41	80	25	Absent	1.2	1.7
2	5/F	L	35	90	60	Absent	0.7	1.9
3	8/F	R	59	–	70	Absent	0.5	1.7
4	8/M	R	38	–	90	Normal	1.3	2.0
5	13/F	L	59	–	50	Absent	1.0	2.1
6	4/F	R	40	60	–	Absent	0.3	1.8

–, not evaluated; ABR, auditory brainstem response; CNC, cochlear nerve canal; DPOAE, distortion product otoacoustic emission; F, female; M, male.

of the affected ears in the remaining six (24%) cases were <60 dB (Table I). These six patients were therefore included in this study for further analysis.

The six pediatric cases consisted of one boy and five girls with a mean age of 7.3 years (range, 4–13 years). None of the children had known syndromes that could cause hearing loss or risk factors of hearing loss such as a history of prematurity, hypoxia, and hyperbilirubinemia.

Imaging

High-resolution computed tomography (HRCT) of the temporal bone in all patients was performed with

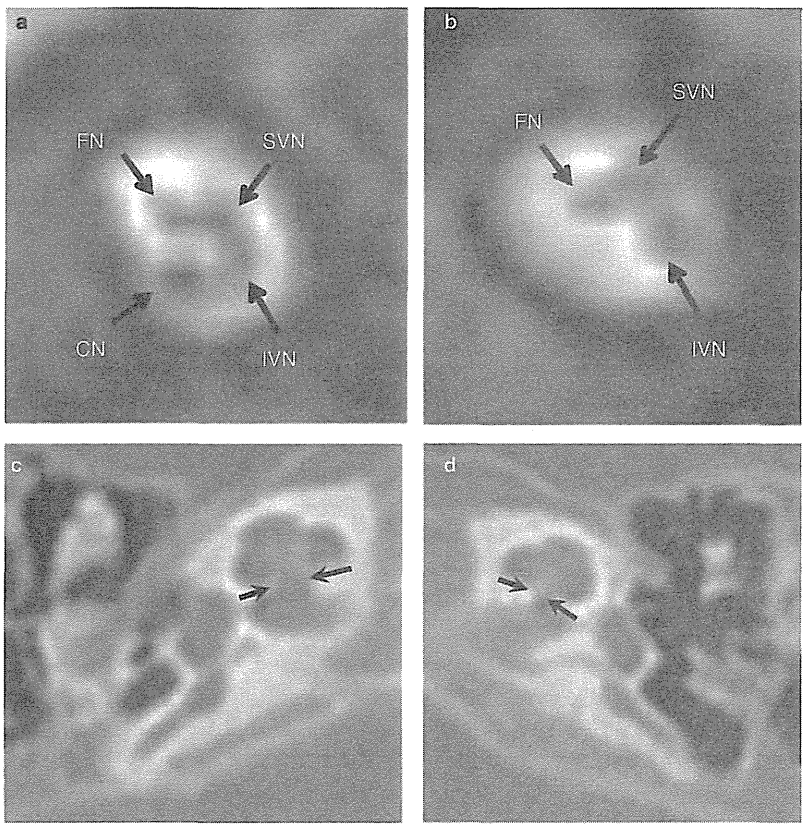

Figure 1. Cochlear nerve hypoplasia in a 5-year-old girl with left sensorineural hearing loss (SNHL) (case 2). (a, b) Oblique sagittal magnetic resonance (MR) images of the inner auditory canal (IAC). Four nerves were detected in the right (a), while the left cochlear nerve is not visible (b). CN, cochlear nerve; FN, facial nerve; IVN, inferior vestibular nerve; SVN, superior vestibular nerve. (c, d) Axial images of temporal bone high-resolution computed tomography (HRCT) show narrowing of left cochlear nerve canal (CNC) (d, 0.7 mm) compared with the right CNC (c, 1.9 mm).

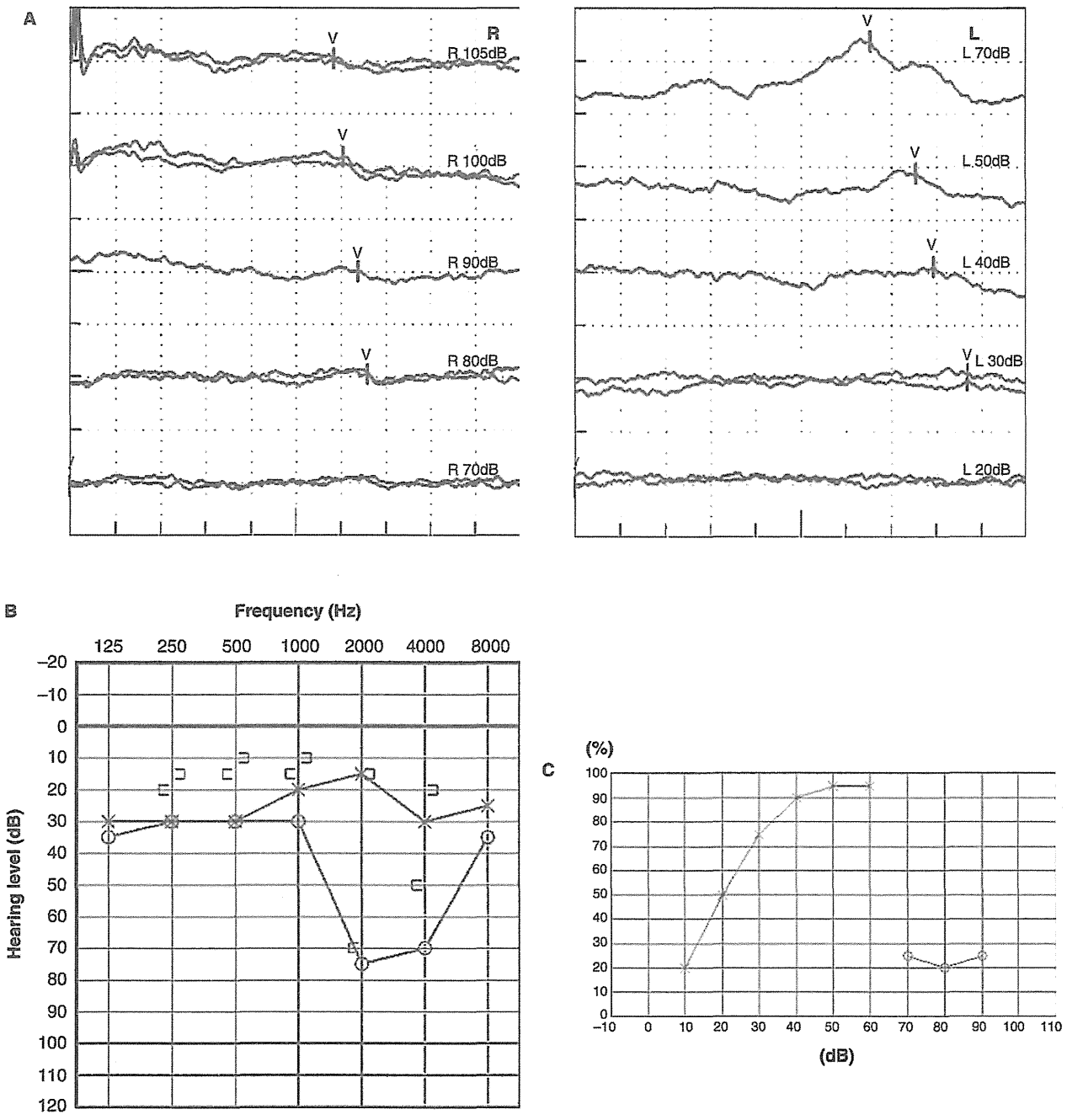

Figure 2. Audiologic findings in a child with right-sided cochlear nerve hypoplasia (case 1). (A) Auditory brainstem responses (ABRs), (B) pure-tone audiogram, (C) word recognition curve.

a multidetector-row CT scanner (8-detector, Lightspeed Ultra, GE, Milwaukee, USA). Images were acquired in the direct axial planes using a 0.652 mm slice thickness. The diameter of the CN canal (CNC) was measured along the inner margin of its bony walls at its middle portion on the axial image of the base of the modiolus.

MR images were obtained using a 1.5 Tesla system (Intera 1.5T; Philips, Belgium) according to a protocol described previously in detail [4]. The MRI scans included 3-D T2-weighted fast spin-echo sequences in axial and oblique sagittal images of the IAC with a 0.7 mm slice thickness. The 3-D constructive interference in steady-state (CISS) images was then reconstructed by traversing the IAC in a perpendicular orientation, producing images that visualized the four nerves (facial, superior vestibular, inferior vestibular, and cochlear). The

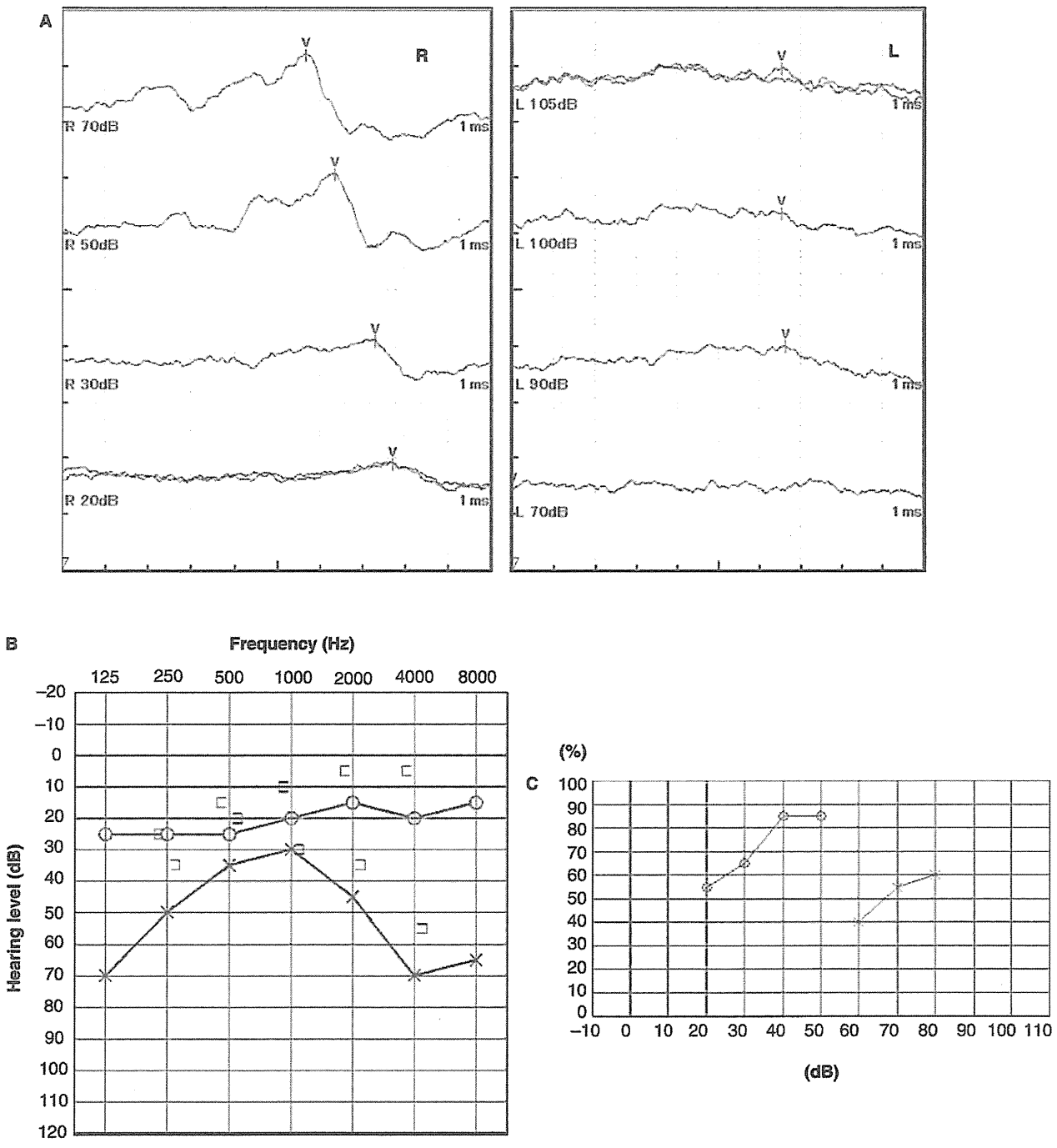

Figure 3. Audiologic findings in a child with left-sided cochlear nerve hypoplasia (case 2). (A) Auditory brainstem responses (ABRs), (B) pure-tone audiogram, (C) word recognition curve.

findings of a normal ear are shown in Figure 1a, b, (case 2, right ear).

Audiologic assessment

In addition to the pure-tone hearing test, distortion product otoacoustic emission (DPOAE) and auditory brainstem response (ABR) testing, as well as speech audiometry were performed. DPOAEs were measured in all subjects for pairs of primary tones (f1 and f2), with a fixed ratio of f2/f1 = 1.2, and fixed levels of 65 dB SPL (L1) and 55 dB SPL (L2) using the ILO292 system (Otodynamics, UK). The frequency of f2 was stepped through a range of 1–6 kHz to yield a nine-point DPGram.

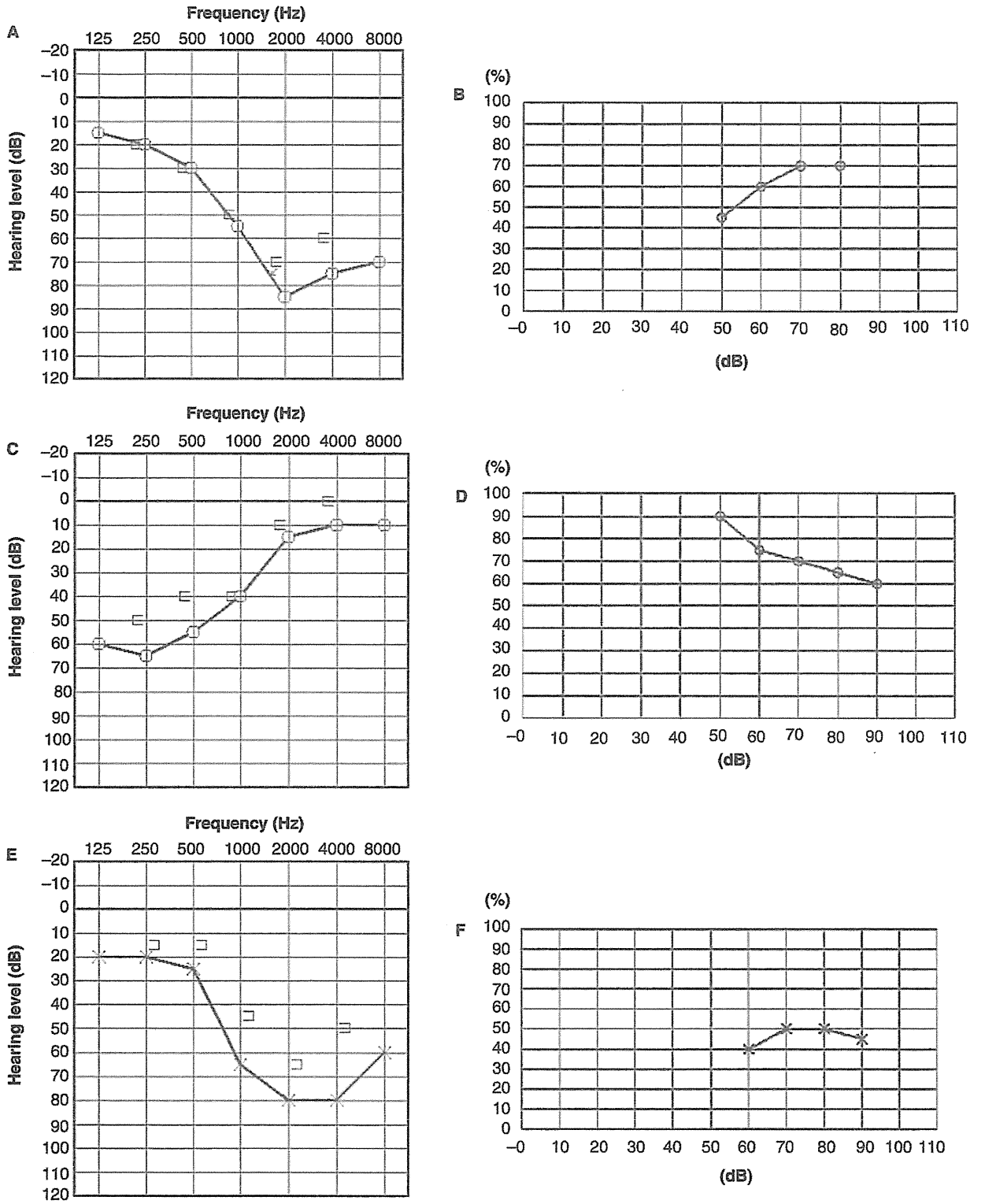

Figure 4. Audiologic findings in ears with cochlear nerve hypoplasia (cases 3–5). (a, c, e) Pure-tone audiograms: (a) case 3, (c) case 4, (e) case 5. (b, d, f) Word recognition curves: (b) case 3, (d) case 4, (f) case 5.

ABRs were recorded in three subjects using the MEB-2204 system (Nihon Koden, Japan). The 0.1 ms clicks with alternating polarity were presented monaurally at a repetition rate of 10 Hz and a maximum intensity of 105 dB nHL.

Speech audiometry was performed in five subjects, but not in case 6 where the test could not be done. The maximum word recognition scores were evaluated based on the percentage of correct answers out of 20 words, using Japanese word list 67-S. In normal-hearing subjects, the maximum word recognition scores using the word list are usually ≥90%.

Results

A summary of the findings for the six children with unilateral CN hypoplasia diagnosed by MRI is shown in Table I. On the oblique sagittal MRI image of case 2, the left CN is undetectable, while the right CN is normal (Figure 1a, b). The hearing levels of the affected ears in the six cases ranged from 35 to 59 dB (Table I). The audiogram shapes (Figures 2, 3, and 4) were high-frequency sloping (cases 3, 5, and 6), rising (case 4), 2–4 kHz notch (case 1), and inverted scoop shape (case 2). DPOAEs were present in only one (17%) of the six affected ears, and the shape of the hearing loss curve for that ear was rising.

In one of the three cases in which ABR testing was performed, the ABR threshold of the ear with CN hypoplasia was significantly elevated compared with that expected from 1000–4000 Hz pure-tone hearing levels (case 2). Speech discrimination tests were performed in five cases (Figures 2c, 3c, and 4b, d, f) but not in the 4-year-old patient (case 6). In two of these five cases (cases 1 and 2), the maximum word recognition scores of the ears with CN hypoplasia were poor compared with those of pure-tone hearing levels. In one case (case 4), the maximum word recognition score of the affected ear was 90%, but the results for 50 dB and 90 dB were 90% and 60%, respectively. Therefore, the word recognition curve in case 4 showed marked roll-over.

The click-evoked ABR tracing, pure-tone audiogram, and word recognition curves for case 1 are shown in Figure 2. The pure-tone audiogram of the right ear (affected side) showed a 2–4 kHz notch configuration. The wave V threshold of the right ear was elevated (80 dB nHL). The ABR threshold compared with the 1–4 kHz pure-tone hearing level of the right ear was slightly higher than expected. The maximum word recognition score of the right ear was 25%, which was lower than expected for pure-tone hearing.

The click-evoked ABR tracing, pure-tone audiogram, and word recognition curves for case 2 are shown in Figure 3. The pure-tone audiogram of the left ear (affected side) showed an inverted scoop shape. The ABR threshold of the left ear was 90 dB nHL and the maximum word recognition score of the left ear was 60%. These values were smaller than expected for pure-tone hearing.

All six ears with CN hypoplasia were associated with CNC stenosis (CNC diameter, <1.5 mm; mean, 0.83 mm). In contrast, the unaffected ears of the six children had CNC diameters of >1.5 mm (mean, 1.9 mm). Axial HRCT images of a representative case (case 2) of severe CNC stenosis are shown in Figure 1c and d. No cochlear malformations were seen in the six children.

Discussion

We defined CN hypoplasia as an undetectable CN on axial, coronal, or reconstructed oblique sagittal MR images. An extremely small nerve, below the limits of resolution of MRI, could appear absent and therefore should not be disregarded. Therefore, we avoid the terms deficiency, aplasia, and agenesis.

The mechanism of CN hypoplasia in children remains speculative. Both congenital deficiency and acquired degeneration of the CN might be seen in children with SNHL [5]. In pediatric cases, it is possible that a vascular insult during critical periods in development may result in isolated CN agenesis or degeneration [1]. CN hypoplasia is often associated with cochlear anomalies [4] or various coexisting syndromes such as CHARGE association [1]. Neither cochlear malformations nor known syndromes were recognized in the patients presented in this report.

CN hypoplasia is not as uncommon as previously thought [1]. Recent studies suggest that CN dysfunction accounts for up to 10% of diagnosed cases of pediatric SNHL [2]. Miyasaka et al. [4] reported CN hypoplasia in 8 of 42 (19%) ears on MRI. Of these, four ears had inner ear malformations. In the present study, no cochlear malformations were recognized in the six ears with CN hypoplasia. In addition, a relationship between CNC stenosis and CN hypoplasia was previously reported [2,6,7]. CNC diameter measurements of <1.8 mm were considered moderate stenosis, while measurements of <1.0 mm were defined as critical stenosis [8]. A CNC diameter of <1.5 mm on CT suggested CN hypoplasia [4,6,7]. All six ears with CN hypoplasia in this study were associated with CNC stenosis (CNC diameter, <1.5 mm). And also 11 ears with CN hypoplasia with profound hearing loss were associated with CNC stenosis. The mean (SD) CNC diameter was 0.83 (0.40) mm in the affected side of 6 cases with mild to moderate hearing loss, and 0.72 (0.32) mm in the affected side of 11 cases with profound hearing

loss. The CNC diameters in the group with profound hearing loss were slightly narrower than in the group with mild to moderate hearing loss, but there was no statistically significant difference ($p = 0.28$, t test). CNC may require stimulation by its contents for normal development, meaning that CNC stenosis may occur secondary to CN hypoplasia [6]. However, it was previously reported that CNC stenosis can occur without CN hypoplasia [4]. CNC stenosis on CT may therefore be indicative of the diagnosis of CN hypoplasia, but MRI should be performed to confirm the diagnosis.

In the past, it was thought that CN hypoplasia was always associated with profound SNHL [1], but a case of CN hypoplasia without profound hearing loss was reported recently [3]. In that case, an extremely small, preserved, and partially functional CN was believed to be present in the affected ear [3]. A minimal number of residual CN fibers, which were too small to be detected by MRI, may be enough to deliver sound information without threshold elevation [8].

CN hypoplasia may present as auditory neuropathy spectrum disorder (ANSD) [1,9]. In this study, DPOAEs were detected in one of six cases, which indicated normal outer hair cell function. In the 11 cases of CN hypoplasia with profound hearing loss, DPOAEs at the affected ears were detected in four cases (36%). The presence rates of DPOAEs were supposed not to relate to hearing levels. The reason for absent DPOAEs in cases of mild hearing loss is unclear, but malformations of inner ear microstructures associated with congenital CN hypoplasia are considered to be the cause of absent DPOAEs. The shape of the hearing loss curve in the case with normal DPOAE was rising (Figure 4c), and the pure-tone thresholds at 2–8 kHz were ≤15 dB. The normal DPOAE response in this case is assumed to indicate the preservation of inner ear function at high frequencies.

In case 2, who was one of three cases in which ABR testing was performed, the ABR threshold of the affected ear was significantly elevated compared with that expected from 1–4 kHz pure-tone hearing levels. The elevated ABR threshold in the case suggests disorders of CN synchrony at high frequencies.

Speech discrimination assessments showed poor maximum word recognition scores compared with that expected from pure-tone hearing levels in two affected ears. In addition, the word recognition curve of an affected ear had marked roll-over. The results of the speech discrimination tests suggested retrocochlear disorders in the affected ears. Some of the findings of the ABR and the word recognition tests in CN hypoplasia are consistent with audiologic characteristics of ANSD, which has been reported as retrocochlear hearing loss in CN hypoplasia [1]. It is believed that 6–28% of ANSD cases are due to CN hypoplasia [1,10,11]. CT is recommended for the initial screening of children with SNHL [4]. For children with ANSD, high-resolution MRI of the CN should be performed as the initial imaging study [12]. The results of the present study suggest that the imaging study for the screening of CN hypoplasia is desirable for even mild to moderate hearing loss.

Conclusion

Here, we presented six pediatric cases of CN hypoplasia with mild to moderate hearing loss. Audiologic characteristics of some ears with CN hypoplasia in this study suggested retrocochlear disorders. Even if hearing loss is mild to moderate, the presence of CN hypoplasia associated with retrocochlear disorders should be considered.

Declaration of interest: The authors report no conflicts of interest. The authors alone are responsible for the content and writing of the paper.

References

[1] Buchman CA, Roush PA, Teagle FB, Brown CJ, Zdanski CJ, Grose JH. Auditory neuropathy characteristics in children with cochlear nerve deficiency. Ear Hear 2006; 27:399–408.

[2] Adunka OF, Roush PA, Teagle HF, Brown CJ, Zdanski CJ, Jewells V, et al. Internal auditory canal morphology in children with cochlear nerve deficiency. Otol Neurotol 2006;27: 793–801.

[3] Miyanohara I, Miyashita K, Takumi K, Nakajo M, Kurono Y. A case of cochlear nerve deficiency without profound sensorineural hearing loss. Otol Neurotol 2011; 32:529–32.

[4] Miyasaka M, Nosaka S, Morimoto N, Taiji H, Masaki H. CT and MR imaging for pediatric cochlear implantation: emphasis on the relationship between the cochlear nerve canal and the cochlear nerve. Pediatr Radiol 2010;40: 1509–16.

[5] Glastonbury CM, Davidson HC, Harnsberger HR, Butker J, Kertesz TR, Shelton C. Imaging findings of cochlear nerve deficiency. AJNR 2002;23:635–43.

[6] Kono T. Computed tomographic features of the bony canal of the cochlear nerve in pediatric patients with unilateral sensorineural hearing loss. Radiat Med 2008;26:115–19.

[7] Komatsubara S, Haruta A, Nagano Y, Kodama T. Evaluation of cochlear nerve imaging in severe congenital sensorineural hearing loss. ORL J Otorhinolaryngol Relat Spec 2007;69:198–202.

[8] Valero J, Blaser S, Papsin BC, James AL, Gordon KA. Electrophysiologic and behavioral outcomes of cochlear implantation in children with auditory nerve hypoplasia. Ear Hear 2012;33:3–18.

[9] O'Leary SJ, Gibson WP. Surviving cochlear function in the presence of auditory nerve agenesis. J Laryngol Otol 1999; 113:1008–10.

[10] Walton J, Gibson WP, Sanli H, Prelog K. Predicting cochlear implant outcomes in children with auditory neuropathy. Otol Neurotol 2008;29:302–9.
[11] Teagle HF, Roush PA, Woodard JS, Hatch DR, Zdanski CJ, Buss E, et al. Cochlear implantation in children with auditory neuropathy spectrum disorder. Ear Hear 2010;31:325–35.
[12] Roche JP, Huang BY, Castillo M, Bassim MK, Adunka OF, Buchman CA. Imaging characteristics of children with auditory neuropathy spectrum disorder. Otol Neurotol 2010;31:780–8.

Otol Neurotol. 2013 Apr;34(3):554-558.

Cochlear Nerve Deficiency and Associated Clinical Features in Patients With Bilateral and Unilateral Hearing Loss.

Nakano A, Arimoto Y, Matsunaga T.

*Division of Otolaryngology, Chiba Children's Hospital, Chiba, Japan, and †Department of Otolaryngology, National Hospital Organization, Tokyo Medical Center, Tokyo, Japan.

Abstract

OBJECTIVE: To clarify the prevalence and clinical characteristics of cochlear nerve deficiency (CND) in patients with congenital bilateral and unilateral hearing loss.

STUDY DESIGN: Retrospective case review.

SETTING: Tertiary referral center.

PATIENTS: One hundred fourteen children with bilateral and 56 children with congenital unilateral sensoneural hearing loss.

MAIN OUTCOME MEASURES: Review of medical records, audiologic tests, and imaging studies. Imaging studies were evaluated for the presence or absence of abnormalities in the bony cochlear nerve canal (BCNC), internal auditory canal (IAC), and inner ear.

RESULTS: The prevalence of CND, whether unilateral or bilateral, was much higher in the unilateral than in the bilateral hearing loss group: 50% (28/56) versus 5.3% (6/114). Among the 6 children with bilateral hearing loss and CND, 2 had bilateral BCNC stenosis alone, 2 had bilateral BCNC stenosis and unilateral IAC stenosis, 1 had unilateral BCNC stenosis alone, and 1 had unilateral IAC stenosis alone. All 28 children with unilateral hearing loss and CND had BCNC stenosis, whereas 9 (32.1%) also had concurrent IAC stenosis. Three of the 6 children with CND and bilateral hearing loss and 5 of the 28 children with CND and unilateral hearing loss also had other inner ear abnormalities.

CONCLUSION: Our results suggest differences in the causes and mechanisms of CND in children with bilateral versus unilateral hearing loss.

PMID: 23449441 [PubMed - as supplied by publisher]

Gene 501 (2012) 193–197

Contents lists available at SciVerse ScienceDirect

Gene

journal homepage: www.elsevier.com/locate/gene

Comorbidity of *GJB2* and *WFS1* mutations in one family

Shujiro B. Minami [a,b,*], Sawako Masuda [c], Satoko Usui [c], Hideki Mutai [b], Tatsuo Matsunaga [a,b]

[a] NHO Tokyo Medical Center, Department of Otolaryngology, Japan
[b] NHO Tokyo Medical Center, National Institute of Sensory Organs, Laboratory of Auditory Disorders, Japan
[c] NHO Mie Hospital, Department of Otolaryngology, Japan

ARTICLE INFO

Article history:
Accepted 22 March 2012
Available online 31 March 2012

Keywords:
Connexin 26
Hereditary hearing loss
Wolframin
DFNB1
DFNA6/14

ABSTRACT

It is rarely reported that two distinct genetic mutations affecting hearing have been found in one family. We report on a family exhibiting comorbid mutation of *GJB2* and *WFS1*. A four-generation Japanese family with autosomal dominant sensorineural hearing loss was studied. In 7 of the 24 family members, audiometric evaluations and genetic analysis were performed. We detected A-to-C nucleotide transversion (c.2576G>C) in exon 8 of *WFS1* that was predicted to result in an arginine-to-proline substitution at codon 859 (R859P), G-to-A transition (c.109G>A) in exon 2 of *GJB2* that was predicted to result in a valine-to-isoleucine substitution at codon 37 (V37I), and C-to-T transition (c.427C>T) in exon 2 of *GJB2* that was predicted to result in an arginine-to-tryptophan substitution at codon 143 (R143W). Two individuals who had heterozygosity of *GJB2* mutations and heterozygosity of *WFS1* mutations showed low-frequency hearing loss. One individual who had homozygosity of *GJB2* mutation without *WFS1* mutation had moderate, gradual high tone hearing loss. On the other hand, a moderate flat loss configuration was seen in one individual who had compound heterozygosity of *GJB2* and heterozygosity of *WFS1* mutations. Our results indicate that the individual who has both *GJB2* and *WFS1* mutations can show *GJB2* phenotype.

1. Introduction

More than half the incidence of congenital hearing loss is due to hereditary factors (Smith et al., 2005). Owing to recent advances in molecular genetics, more than 400 genetic syndromes have been associated with hearing loss and more than 140 genetic loci associated with nonsyndromic hearing loss have been mapped, with more than 60 genes identified to date (Van Camp G, Smith RJH. Hereditary Hearing Loss Homepage, last updated 2011 June 17. Available at: http://hereditaryhearingloss.org). Hereditary hearing loss can be inherited as an autosomal dominant, autosomal recessive, X-linked or mitochondrial (maternally inherited) condition. It is rarely reported that two distinct genetic mutations linked to hearing loss have been found in one family. Now we report on a family exhibiting comorbid mutations of *GJB2* and *WFS1*.

Mutations in the *GJB2* gene encoding connexin 26 are the most common cause of nonsyndromic autosomal recessive sensorineural hearing loss (DFNB1) in many populations (Estivill et al., 1998; Matsunaga et al., 2006; Morell et al., 1998). To date, more than 150 mutations, polymorphisms, and unclassified variants have been described in the *GJB2* gene (http://davinci.crg.es/deafness). The mutation spectrum and prevalence of mutations vary significantly across different ethnic groups (Dai et al., 2009; Estivill et al., 1998; Morell et al., 1998; Ohtsuka et al., 2003). SNHL-causing allele variants of *GJB2* alter the function of the encoded protein, connexin 26, in the inner ear. Connexin 26 aggregates in groups of six around a central 2–3 nm pore to form a doughnut-shaped structure called a connexon (Maeda et al., 2009). The connexons from contiguous cells covalently bond to form intercellular channels. Aggregations of connexons are called plaques and are the constituents of gap junctions. The gap junction system might be involved in potassium circulation, allowing ions that enter hair cells during mechanosensory transduction to be recycled to the stria vascularis (Zdebik et al., 2009).

The *WFS1* gene maps to chromosome 4p16, and has a transcript of 3640 nucleotides of which 2673 bp are coding. *WFS1* consists of 8 exons, of which the first exon is non-coding. The largest exon is exon 8, where the coding part is 1812 bp long. Numerous sequence variants/polymorphisms, mainly in exon 8 of *WFS1*, have been reported (Cryns et al., 2003a). *WFS1* extends over 33.4 kb of genomic DNA. The gene transcribes an mRNA of 3.6 kb that encodes wolframin, an 890-amino-acid protein with a predicted molecular mass of 100 kDa (Inoue et al., 1998). Its function within the inner ear is currently unknown, but its localization in the endoplasmic reticulum (ER) suggests a possible role for wolframin in ion homeostasis maintained by the canalicular reticulum, a specialized form of ER (Cryns et al., 2003b). Mutations in *WFS1* underlie autosomal recessive Wolfram syndrome (MIM# 222300) (Strom et al., 1998) and autosomal dominant low frequency sensorineural

Abbreviations: ABRs, Auditory Brainstem Responses; ASSR, Auditory Steady-State Response.

* Corresponding author at: 2-5-1 Higashigaoka Meguro-ku, Tokyo 152-8902, Japan. Tel.: +81 3 3411 0111; fax: +81 3 3412 9811.
E-mail address: shujirominami@me.com (S.B. Minami).

0378-1119/$ – see front matter © 2012 Elsevier B.V. All rights reserved.
doi:10.1016/j.gene.2012.03.060

hearing impairment (LFSNHI) DFNA6/14 (MIM# 600965) (Bespalova et al., 2001; Young et al., 2001). Hearing impairment in Wolfram syndrome is progressive and mainly affects the high frequencies (Higashi, 1991). In contrast, hearing impairment associated with DFNA6/14 affects only the low frequencies and it shows little or no progression (Bom et al., 2002; Brodwolf et al., 2001; Kunst et al., 1999; Lesperance et al., 2003; Pennings et al., 2003). This is the first report of a family with comorbid hereditary hearing loss of DFNB1 and DFNA6/14.

2. Materials and methods

2.1. Family report

All the procedures were approved by the Ethics Review Committee of National Tokyo Medical Center and were carried out only after a written informed consent had been obtained from each individual or parents of the children.

A four-generation Japanese family with autosomal dominant sensorineural hearing loss was studied (Fig. 1). The family does not have a history of diabetes mellitus, dysopia, nor psychiatric disorders, which are the characteristic symptoms of Wolfram syndrome. In 7 of the 23 family members, audiometric evaluations and a genetic analysis were performed. Information regarding hearing loss in the other 16 family members was obtained through interviews with the 7 family members. Pure tone audiometry was carried out in all participants, with the exception of the proband, who was 1 year of age. Hearing loss in the proband was assessed via Auditory Brainstem Responses (ABRs) and Auditory Steady-State Response (ASSR). During the recording sessions for evoked audiometry (ABR and ASSR), the patient was in a state of induced sleep. He was sedated with triclofos sodium (80 mg/kg, administered orally). ABR and ASSR studies were obtained using the AUDERA device (Grason-Stadler).

2.2. Genetic analysis

Based on the age and audiometric configurations of the family members, we screened for the presence of *GJB2* and *WFS1* mutations (Matsunaga, 2009). The entire coding regions of*GJB2* were amplified using the primer pair Cx48U/Cx1040L (Matsunaga et al., 2006). Coding exons 2–7 of WFS1 were amplified using primers and the PCR protocol previously described (Strom et al., 1998). For the coding sequence in exon 8 of *WFS1*, three primer pairs were designed, yielding overlapping products of around 700 base pairs. The primer pairs are as follows: 5′-AGGCGTGAGATGGGAGCAGT-3′ and 5′-AGGCGTGAGATGGGAGCAGT-3′, 5′-TGGTGTGCTTCATGTGGTG-3′ and 5′-TGGCATGCCCACGGTAATCT-3′, 5′-ATCGTGCTGTTCTGCTGGTTC-3′ and 5′-ACACATGGTCGCAAGGTCTC-3′. Polymerase chain reaction products were sequenced and analyzed with an ABI sequencer 377XL (PerkinElmer).

3. Results

Individual IV-3 is the proband, a 1-year-old boy. He was born a low-birth-weight baby (1861 g) after a gestation of 30 weeks and 6 days, and admitted to a neonatal intensive care unit. He underwent the ABR test at 8-months-old and the wave V in responses to click noises of 40 dB on both sides was confirmed (Figs. 2A,B). ASSR test at one year of age showed a low-frequency hearing loss (Figs. 2C,D). In the proband, we detected a heterozygous A-to-C nucleotide transversion (c.2576G>C) in exon 8 of *WFS1* that was predicted to result in an arginine-to-proline substitution at codon 859 (R859P), which was reported as a pathological mutation. The proband also had a heterozygous G-to-A transition (c.109G>A) in exon2 of *GJB2* that was predicted to result in avaline-to-isoleucine substitution at codon 37 (V37I). Individual IV-2 had low frequency sensorineural hearing loss with pure tone audiometry at 4 years of age as well (Fig. 3A). Sequencing of *GJB2* and *WFS1* revealed a heterozygous C-to-T transition (c.427C>T) in exon2 of *GJB2* that was predicted to result

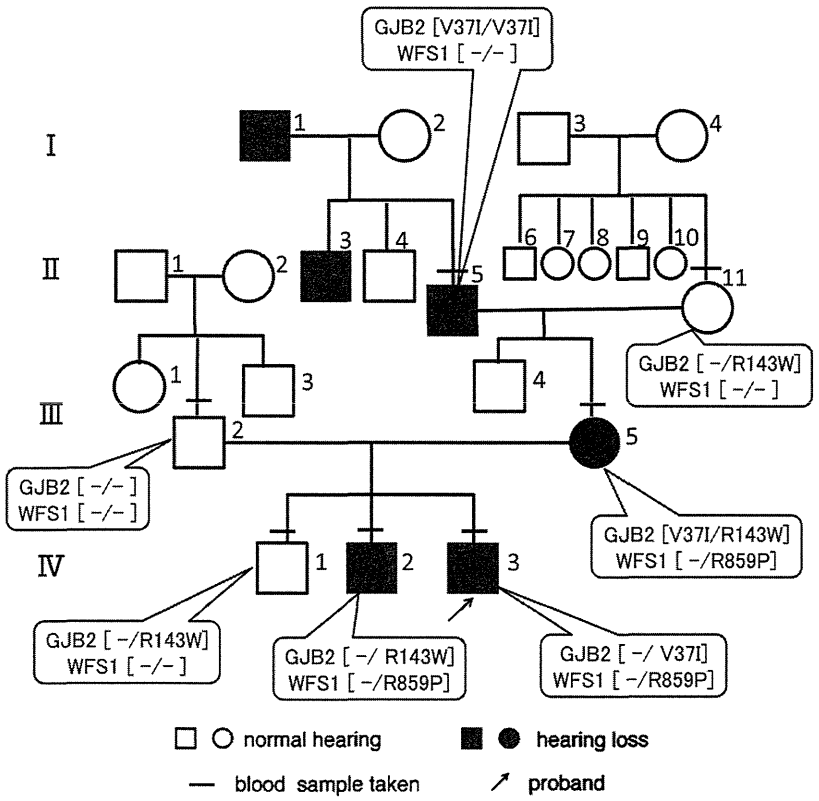

Fig. 1. Pedigree of the DFNB1/DFNA6/14 family.

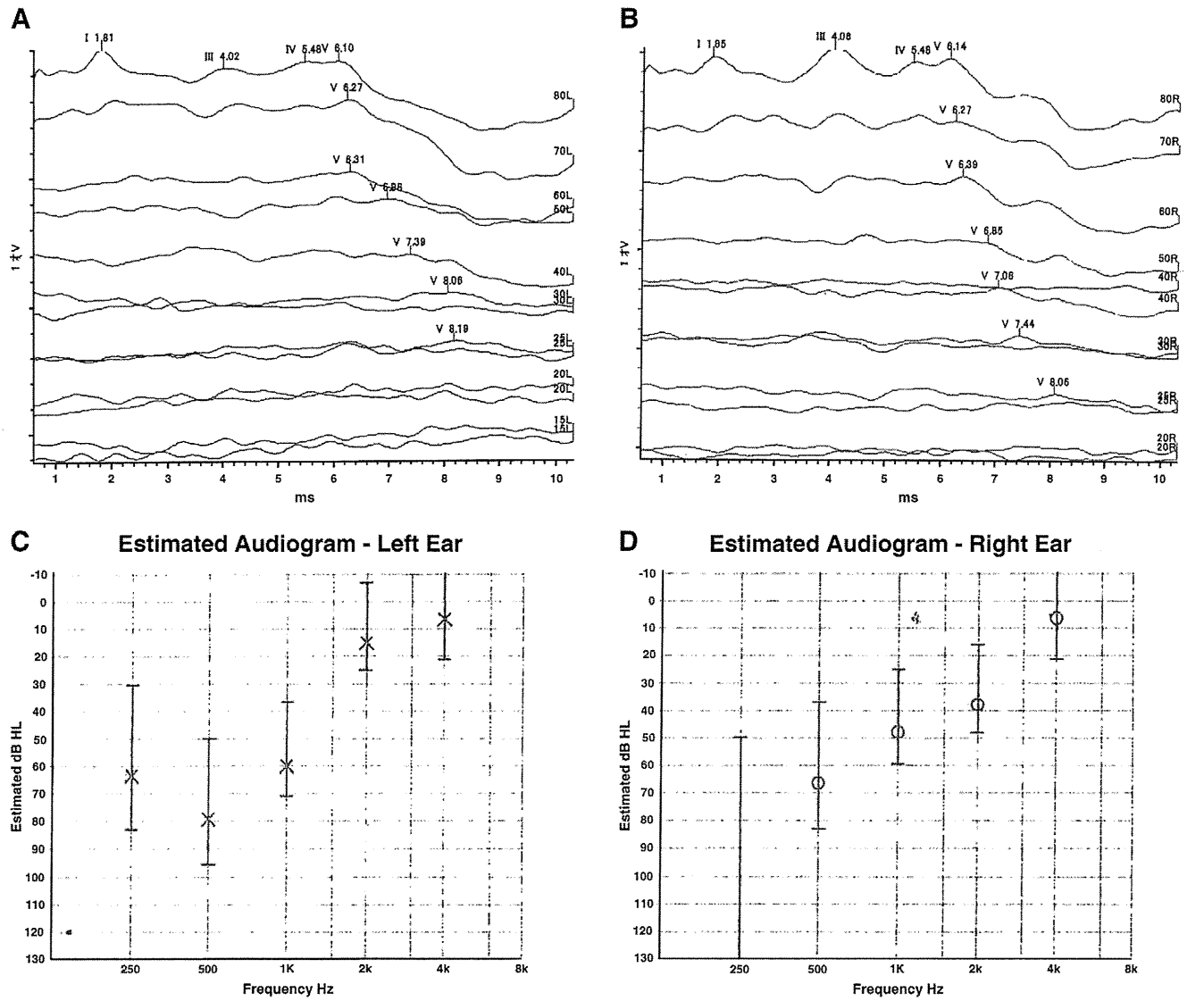

Fig. 2. Auditory assessment of individual IV-3 (proband). Both sides of ABRs (A: left, B: right) showing well waveforms at wave V down to 40 dB. The estimated audiograms by ASSR (C: left, D: right) show reverse-slope hearing loss.

in an arginine-to-tryptophan substitution at codon 143 (R143W) and heterozygosity for R859P mutation of *WFS1*. Individual IV-1 had normal hearing and just heterozygosity for the R143W mutation of GSB2. Individual III-2 had normal hearing and no mutations of *GJB2* and *WFS1*. Individual III-5 was 34 years old, and had moderate sensorineural hearing impairment at all frequency levels (Fig. 3B). Sequencing of *GJB2* and *WFS1* revealed compound heterozygosity for the V37I and R143W mutation of *GJB2* and heterozygosity for R859P mutation of *WFS1*. Individual II-5 was 61 years old, and had moderate hearing loss gently sloping (Fig. 3C). Sequencing of *GJB2* and *WFS1* revealed homozygosity for the V37I mutation of GJB2, but not *WFS1* mutations. Individual II-11 had normal hearing and heterozygosity for the R143W mutation of GJB2.

4. Discussion

We found a family who has both a *GJB2* mutation and a *WFS1* mutation. The individuals who have heterozygosity of *GJB2* mutations and heterozygosity of *WFS1* mutations show low-frequency hearing loss. On the other hand, flat loss configuration was found in the individual who has compound heterozygosity of *GJB2* mutation and *WFS1* mutation, and gradual high tone loss was seen in the individual who has homozygosity of *GJB2* mutation without *WFS1* mutations. According to our results, the individual who has both *GJB2* and *WFS1* mutations shows the *GJB2* phenotype. We should think about the effect of age modifying the hearing phenotype. However, the hearing impairments of III-5, 34 years old woman, andII-5, 61 years old man, are much worse at all frequencies than ISO 7029 norms, which were applied to establish 95th percentile threshold values for presbyacusis at each frequency in relation to the patient's age and sex (ISO 7029–2000 [ISO, 2000]).

Both V37I and R143W mutations in *GJB2* are non-inactivating mutations (Snoeckx et al., 2005). It has been reported that non-inactivating mutations of *GJB2* show less severe hearing impairment than inactivating mutations (Angeli, 2008; Cryns et al., 2004). As in this report, both homozygosity of V37I mutation and compound heterozygosity of V37I and R143W mutations show moderate hearing impairment, even if they are comorbid with *WFS1* mutation.

Both parents of subject III-5 had no *WFS1* mutations, indicating that heterozygosity for R859P mutation of *WFS1* of individual III-5 is a new mutation. R859P mutation of *WFS1*has been previously reported in one large family from the United States (Gurtler et al., 2005). A missense mutation at c.2576G>C results in an amino acid substitution, p.R859P, in a highly conserved area across human, mouse, and

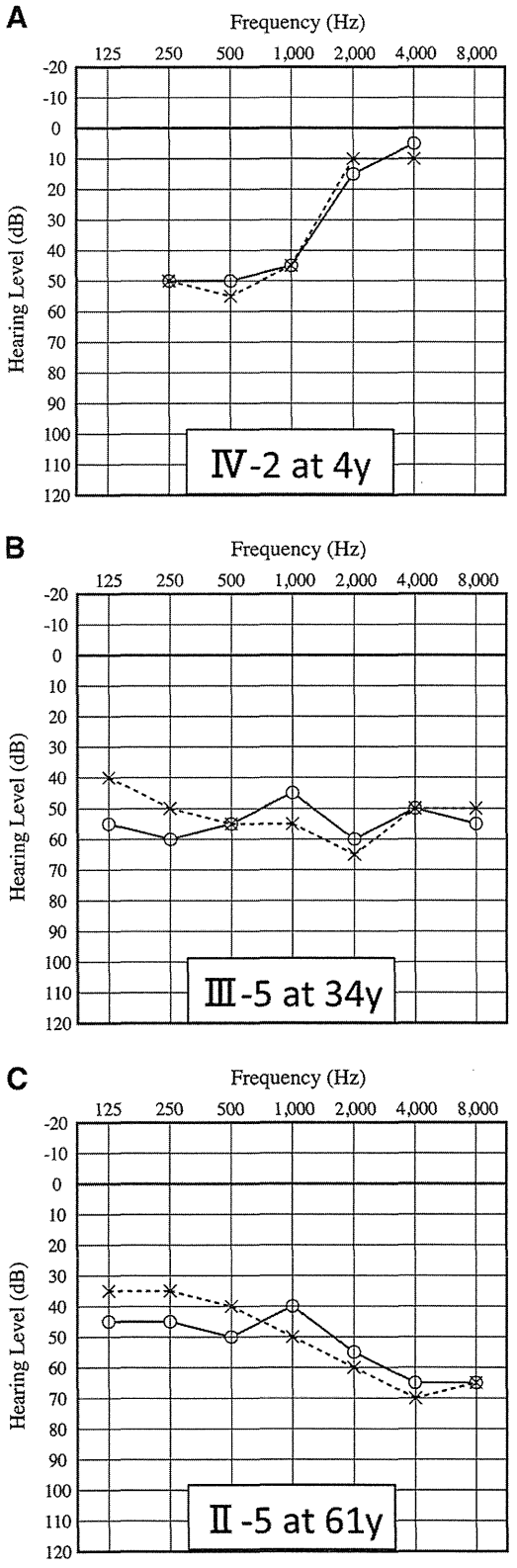

Fig. 3. Representative audiograms of individual IV-2 (A), individual III-5 (B), and individual II-5 (C) showing pure-tone audiometry results for air conduction bilaterally. Circles, air conduction right ear; crosses, air conduction left ear. Severe reverse-slope loss is seen in IV-2, whereas moderate flat hearing loss in III-5 and moderate hearing loss with mild ski-slope type inII-5.

rat. The mutation substitutes proline for naturally occurring arginine; this substitution is known to disrupt helical chains. It is likely that the mutation significantly alters the secondary structure of wolframin by creating a bending point in the amino acid chain in the C-terminal domain. The wolframin function in the cochlea is unknown so far, but if wolframin and connexin 26 serve very different functions in the cochlea, the person who has comorbid *WFS1* and GSB2 mutations would show additive hearing impairment. However, the comorbid case showed non-additive hearing loss, which indicates that wolframin may play a relevant role with connexin 26. That is to say, it is possible that wolframin in the cochlea works in potassium recycling. It is reported that sodium–potassium ATPase b1 subunit is a molecular partner of wolframin (Zatyka et al., 2008), which may support our hypothesis. However, genotype and phenotype correlation may not be such a simple process, but there may be many genetic and environmental factors. The duality of *WFS1* in frequency-specific hearing, which is the observation that recessive inactivating mutations cause high-frequency hearing loss as part of Wolfram syndrome and dominant noninactivating missense mutations cause low-frequency hearing loss, is still mysterious.

In conclusion, we have reported on a family which has comorbid mutations of *GJB2* and *WFS1* mutations, including one individual who has both *GJB2* and *WFS1* mutations and shows a *GJB2* phenotype. We should think about the possibility of comorbid gene mutation for hearing impairment. It is worth noting that more than 2 genetic mutations responsible for deafness can occur in one individual, and that the hearing characteristics of phenotype help us to speculate on molecular functions in the cochlea.

Acknowledgments

This work was supported by JSPS KAKENHI 22791627 and a Grant-in-Aid for Clinical Research from the National Hospital Organization.

References

Angeli, S.I., 2008. Phenotype/genotype correlations in a DFNB1 cohort with ethnical diversity. Laryngoscope 118, 2014–2023.
Bespalova, I.N., et al., 2001. Mutations in the Wolfram syndrome 1 gene (WFS1) are a common cause of low frequency sensorineural hearing loss. Hum. Mol. Genet. 10, 2501–2508.
Bom, S.J., Van Camp, G., Cryns, K., Admiraal, R.J., Huygen, P.L., Cremers, C.W., 2002. Autosomal dominant low-frequency hearing impairment (DFNA6/14): a clinical and genetic family study. Otol. Neurotol. 23, 876–884.
Brodwolf, S., Boddeker, I.R., Ziegler, A., Rausch, P., Kunz, J., 2001. Further evidence for linkage of low–mid frequency hearing impairment to the candidate region on chromosome 4p16.3. Clin. Genet. 60, 155–160.
Cryns, K., et al., 2003a. Mutational spectrum of the WFS1 gene in Wolfram syndrome, nonsyndromic hearing impairment, diabetes mellitus, and psychiatric disease. Hum. Mutat. 22, 275–287.
Cryns, K., et al., 2003b. The WFS1 gene, responsible for low frequency sensorineural hearing loss and Wolfram syndrome, is expressed in a variety of inner ear cells. Histochem. Cell Biol. 119, 247–256.
Cryns, K., et al., 2004. A genotype—phenotype correlation for GJB2 (connexin 26) deafness. J. Med. Genet. 41, 147–154.
Dai, P., et al., 2009. GJB2 mutation spectrum in 2,063 Chinese patients with nonsyndromic hearing impairment. J. Transl. Med. 7, 26.
Estivill, X., et al., 1998. Connexin-26 mutations in sporadic and inherited sensorineural deafness. Lancet 351, 394–398.
Gurtler, N., et al., 2005. Two families with nonsyndromic low-frequency hearing loss harbor novel mutations in Wolfram syndrome gene 1. J. Mol. Med. 83, 553–560.
Higashi, K., 1991. Otologic findings of DIDMOAD syndrome. Am. J. Otol. 12, 57–60.
Inoue, H., et al., 1998. A gene encoding a transmembrane protein is mutated in patients with diabetes mellitus and optic atrophy (Wolfram syndrome). Nat. Genet. 20, 143–148.
ISO (International Organization for Standardization), 2000. ISO 7029-2000: Acoustics—Statistical Distribution of Hearing Thresholds as a Function of Age, 2nd ed. International Organization for Standardization, Geneva.
Kunst, H., Marres, H., Huygen, P., Van Camp, G., Joosten, F., Cremers, C., 1999. Autosomal dominant non-syndromal low-frequency sensorineural hearing impairment linked to chromosome 4p16 (DFNA14): statistical analysis of hearing threshold in relation to age and evaluation of vestibulo-ocular functions. Audiology 38, 165–173.
Lesperance, M.M., Hall III, J.W., San Agustin, T.B., Leal, S.M., 2003. Mutations in the Wolfram syndrome type 1 gene (WFS1) define a clinical entity of dominant

low-frequency sensorineural hearing loss. Arch. Otolaryngol. Head Neck Surg. 129, 411–420.
Maeda, S., et al., 2009. Structure of the connexin 26 gap junction channel at 3.5 A resolution SUPPLEMENTARY INFORMATION. Nature 458, 597–602.
Matsunaga, T., 2009. Value of genetic testing in the otological approach for sensorineural hearing loss. Keio J. Med. 58, 216–222.
Matsunaga, T., Hirota, E., Bito, S., Niimi, S., Usami, S., 2006. Clinical course of hearing and language development in GJB2 and non-GJB2 deafness following habilitation with hearing aids. Audiol. Neurootol. 11, 59–68.
Morell, R.J., et al., 1998. Mutations in the connexin 26 gene (GJB2) among Ashkenazi Jews with nonsyndromic recessive deafness. N. Engl. J. Med. 339, 1500–1505.
Ohtsuka, A., et al., 2003. GJB2 deafness gene shows a specific spectrum of mutations in Japan, including a frequent founder mutation. Hum. Genet. 112, 329–333.
Pennings, R.J., et al., 2003. Progression of low-frequency sensorineural hearing loss (DFNA6/14-WFS1). Arch. Otolaryngol. Head Neck Surg. 129, 421–426.
Smith, R.J., Bale Jr., J.F., White, K.R., 2005. Sensorineural hearing loss in children. Lancet 365, 879–890.
Snoeckx, R.L., et al., 2005. GJB2 mutations and degree of hearing loss: a multicenter study. Am. J. Hum. Genet. 77, 945–957.
Strom, T.M., et al., 1998. Diabetes insipidus, diabetes mellitus, optic atrophy and deafness (DIDMOAD) caused by mutations in a novel gene (wolframin) coding for a predicted transmembrane protein. Hum. Mol. Genet. 7, 2021–2028.
Young, T.L., et al., 2001. Non-syndromic progressive hearing loss DFNA38 is caused by heterozygous missense mutation in the Wolfram syndrome gene WFS1. Hum. Mol. Genet. 10, 2509–2514.
Zatyka, M., et al., 2008. Sodium–potassium ATPase 1 subunit is a molecular partner of wolframin, an endoplasmic reticulum protein involved in ER stress. Hum. Mol. Genet. 17, 190–200.
Zdebik, A.A., Wangemann, P., Jentsch, T.J., 2009. Potassium ion movement in the inner ear: insights from genetic disease and mouse models. Physiology (Bethesda) 24, 307–316.

Biochemical and Biophysical Research Communications 432 (2013) 475–479

Contents lists available at SciVerse ScienceDirect

Biochemical and Biophysical Research Communications

journal homepage: www.elsevier.com/locate/ybbrc

Moderate hearing loss associated with a novel KCNQ4 non-truncating mutation located near the N-terminus of the pore helix

Takahisa Watabe [a], Tatsuo Matsunaga [b,*], Kazunori Namba [b], Hideki Mutai [b], Yasuhiro Inoue [a], Kaoru Ogawa [a]

[a] Department of Otolaryngology, Head and Neck Surgery, Keio University, School of Medicine, 35 Shinanomachi, Shinjuku, Tokyo 160-8582, Japan
[b] The Laboratory of Auditory Disorders, National Institute of Sensory Organs, National Tokyo Medical Center, 2-5-1 Higashigaoka, Meguro, Tokyo 152-8902, Japan

ARTICLE INFO

Article history:
Received 28 January 2013
Available online 9 February 2013

Keywords:
KCNQ4
Nonsyndromic hearing loss
Dominant negative effect
Haploinsufficiency
Molecular modeling

ABSTRACT

Genetic mutation is one of the causative factors for idiopathic progressive hearing loss. A patient with late-onset, moderate, and high-frequency hearing loss was found to have a novel, heterozygous *KCNQ4* mutation, c.806_808delCCT, which led to a p.Ser260del located between S5 and the pore helix (PH). Molecular modeling analysis suggested that the p.Ser269del mutation could cause structural distortion and change in the electrostatic surface potential of the *KCNQ4* channel protein, which may impede K+ transport. The present study supports the idea that a non-truncating mutation around the N-terminus of PH may be related to moderate hearing loss.

1. Introduction

Currently, 50 loci and 27 responsible genes for autosomal dominant non-syndromic hearing loss (DFNA) have been identified [1]. *KCNQ4* is one gene that can cause DFNA, type 2 (DFNA2, OMIM: 600101) [2,3]. Patients with mutations in this gene present progressive sensorineural hearing loss starting in the high frequency range. *KCNQ4* (OMIM: 603537) is a voltage-gated KQT-like potassium channel. It modulates the resting membrane potential of the outer hair cells, a type of auditory sensory cell. A functional *KCNQ4* channel consists of four subunits. Each subunit contains six putative domains that span the cellular membrane (S1–S6), a K+-selective pore region consisting of S5, S6, a pore helix (PH), and a pore-loop (P-loop) domain, and N- and C-terminal regions [3].

So far, 11 missense mutations, one nonsense mutation, and three small deletion mutations in *KCNQ4* have been reported to be associated with hearing loss. Understanding the molecular pathology resulting from each *KCNQ4* mutation would be beneficial in predicting the clinical course of KCNQ-related hearing loss. *KCNQ4* mutations can be divided into non-truncating and truncating mutations (Table 1). Most of the *KCNQ4* non-truncating mutations in the pore region are associated with severe hearing loss, except for a non-truncating mutation at the N-terminus of PH, p.Tyr270His, which has been associated with moderate hearing loss [13]. In an electrophysiological study, co-expression of wild-type *KCNQ4* with each non-truncating mutation associated with severe hearing loss, including p.Leu274His, p.Trp276Ser, p.Leu281-Ser, p.Gly285Cys, p.Gly285Ser, p.Gly296Ser, p.Gly321Ser, and p.Gly322_Leu327del, has been shown to result in significantly reduced or non-detectable current [14]. These results indicate that the severe hearing loss in patients carrying these heterozygous mutations is due to a dominant negative effect. On the other hand, the protein products of two *KCNQ4*-truncating mutations, p.Gln71SerfsX138 and p.Gln71fs, lack structural motifs, such as transmembrane domains, and are probably not synthesized from these alleles. Moderate hearing loss in patients carrying these mutations in the heterozygous allele has been considered to be due to haploinsufficiency [3,11].

We identified a novel heterozygous *KCNQ4* non-truncating mutation, c.806_808delCCT, that leads to deletion of a serine residue at position 269 (p.Ser269del), located in the region between S5 and the PH of the protein. Unlike other patients with *KCNQ4* non-truncating mutations, the patient who carried this mutation presented moderate hearing loss. Previously, we reported that a patient having *KCNQ4* with p.Try270His, which is located next to Ser269, showed moderate hearing loss [13], raising the possibility that mutation at or proximal to the N-terminus of PH is associated

Abbreviations: DFNA2, nonsyndromic autosomal dominant sensorineural deafness type 2; *KCNQ4*, potassium voltage-gated channel; KQT-like subfamily, member 4; ABR, auditory brainstem response.

* Corresponding author. Fax: +81 3 3412 9811.
E-mail address: matsunagatatsuo@kankakuki.go.jp (T. Matsunaga).

0006-291X/$ - see front matter © 2013 Elsevier Inc. All rights reserved.
http://dx.doi.org/10.1016/j.bbrc.2013.01.118

Table 1
KCNQ4 mutations affecting the pore region of the channel protein in DFNA2 families.

	Exon		Nucleotide	Amino acid	Protein domain	Onset (y)	Progression	Severity	Mechanism	Refs.
Non-truncating mutation	5	Missense	c.778G>A	p.Glu260Lys	S5	1–20	Yes	SV	Unknown	[9]
	5		c.785A>T	p.Asp262Val	S5-PH	1–20	Yes	SV	Unknown	[9]
	5		c.808T>C	p.Tyr270His	N-terminus of PH	0	Yes	MD	Unknown	[13]
	5		c.821T>A	p.Leu274His	PH	1–20	Yes	SV	D.N.E.	[12]
	5		c.827G>C	p.Trp276Ser	PH	1–20	Yes	SV	D.N.E.	[3–5]
	6		c.842T>C	p.Leu281Ser	PH	1–20	Yes	SV	D.N.E.	[6]
	6		c.853G>T	p.Gly285Cys	P-loop	1–20	Yes	SV	D.N.E.	[3]
	6		c.853G>A	p.Gly285Ser	P-loop	1–20	Yes	SV	D.N.E.	[2]
	6		c.859G>C	p.Gly287Arg	P-loop	1–20	Yes	SV	D.N.E.	[7]
	6		c.886G>A	p.Gly296Ser	S6	1–20	Yes	SV	D.N.E.	[8]
	7		c.961G>A	p.Gly321Ser	S6	1–20	Yes	SV	D.N.E.	[3]
	4	Deletion	c.664_681del18	p.Gly322_Leu327del	S5	1–20	Yes	SV	D.N.E.	[10]
	5		c.806_808del3	p.Ser269del	S5-PH	1–20	Yes	MD	See discussion	This study
Truncating mutation	1	Deletion	c.211del1	p.Gln71SerfsX138	N-terminal cytoplasmic	Unknown	Yes	MD	H.I.?	[11]
	1		c.212_224del13	p.Gln71fs	N-terminal cytoplasmic	1–20	Yes	MD	H.I.?	[3]
	5	Nonsense	c.725G>A	p.Trp242X	S5	1–20	Unknown	SV	Unknown	[9]

SV: severe, MD: moderate D.N.E.: dominant negative effect, H.I.: haploinsufficiency, PH: pore helix.

with moderate hearing loss. In this study, we used molecular modeling to elucidate the molecular mechanism underlying moderate hearing loss associated with *KCNQ4* harboring the p.Ser269del mutation.

2. Materials and methods

2.1. Subjects

All procedures were approved by the Ethics Review Committee of National Mie Hospital and National Tokyo Medical Center, and were conducted after written informed consent had been obtained from each individual.

2.2. Clinical analysis

Hearing level was measured by pure tone audiometry and evaluated by averaging four frequencies, 500, 1000, 2000, and 4000 Hz in the better hearing ear and was classified according to the criteria of GENDEAF (moderate, 41–70 dB; severe, 71–95 dB) [1]. Clinical information, such as age of onset and presence of progression, was gathered from the medical records. Computed tomography (CT) and magnetic resonance imaging (MRI) were done to check whether the patient had an inner ear anomaly and/or retrocochlear disease. Auditory brainstem response (ABR) and distortion product otoacoustic emission (DPOAE) were also examined to evaluate inner ear function.

2.3. Genetic analysis

KCNQ4 was selected as the candidate gene on the basis of clinical features, including onset of hearing loss, audiogram patterns, imaging studies, and hereditary pattern [15]. Prior to this study, the patient was confirmed to have neither GJB2 mutations, the most common causative gene of hereditary hearing loss, nor mitochondrial m.1555A>G and m.3243A>G mutations. Genomic DNA was extracted from blood samples using the Gentra Puregene Blood kit (QIAGEN, Hamburg, Germany). PCR primers specific for *KCNQ4* (GenBank NG_008139, NCBI Build37.1) were selected from the resequencing amplicon probe sets (NCBI). All of the exons, together with the flanking intronic regions, of *KCNQ4* were analyzed by bidirectional sequencing using an ABI 3730 Genetic Analyzer (Applied Biosystems, CA, USA) and the ABI Prism Big Dye Terminator Cycle Sequencing kit (Applied Biosystems). The sequences were characterized using SeqScape software v.2.6 (Applied Biosystems) and DNASIS Pro (Hitachisoft, Tokyo, Japan). Control DNA was obtained from 96 Japanese subjects with normal hearing.

2.4. Molecular model analysis

To predict the effects of the mutation on the KCNQ4 channel, molecular modeling of KCNQ4 was performed as previously described [13]. The crystal structure of Kv1.2 (PDB ID: 3LUT, chain B) [16] was used as the structural template for modeling of the *KCNQ4* sequence based on sequence homology as determined through Gapped BLAST [17] and PDBsum [18]. The pore regions of wild-type KCNQ4 and the p.Ser269del mutation were modeled using SWISS-MODEL Workspace [19] and validated using the Verify 3D Structure Evaluation server [20,21]. The models were each superimposed onto Kv1.2 using Chimera [22] to visualize ribbon models with electrostatic surface potentials and the hydrogen bonds of either wild-type KCNQ4 or KCNQ4 with the p.Ser269del mutation.

3. Results

3.1. Clinical features

The proband was a 25-years-old female in a pedigree of autosomal dominant progressive hearing loss (Fig. 1A). She has become conscious of progressive bilateral hearing loss, since she has become 20 years-old. At 24 years-old, severe mixed hearing loss with high frequency dominance was found in the right ear by pure tone audiometry. An air-bone gap was considered to have resulted from an operation for a right cholesteatoma at 8 years of age. Moderate sensorineural hearing loss with high frequency dominance was found in the left ear (Fig. 1B). No other symptoms accompanying the hearing loss were identified. ABR showed a threshold of 90 dB in the left ear, and no response at 90 dB in the right ear. DPOAE showed a response only at 1000 Hz in the left ear and no response in the right ear. CT and MRI failed to reveal deformity of the inner ear or structural abnormality in the central auditory pathway.

3.2. Novel mutation of KCNQ4

Sequencing analysis of *KCNQ4* from the patient identified a heterozygous deletion of three nucleotides, CCT, at position 806–808 (c.806_808delCCT). The deletion mutation causes a change of amino acid residues from Ser268-Ser269-Tyr270 to Ser268-Tyr269 (p.Ser269del) without a frameshift (Fig. 2A). Ser269 was located

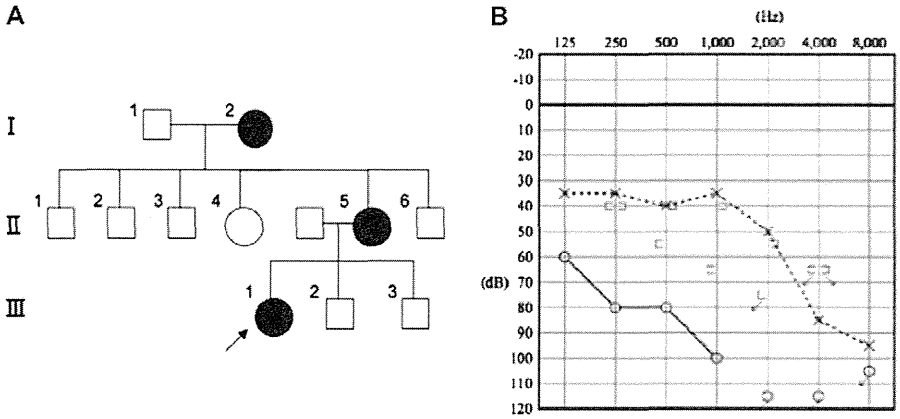

Fig. 1. Clinical information. (A) Pedigree of a family carrying heterozygous *KCNQ4* with the c.806_808delCCT (p.Ser269del) mutation. Individuals with hearing loss are indicated by filled symbols. The arrow indicates the proband. (B) Pure tone audiogram from the proband at 25 years old. Open circles with line: air conduction thresholds of the right ear; x with dotted line: air conduction thresholds of the left ear; left bracket: bone conduction thresholds of the right ear; right bracket: bone conduction thresholds of the left ear. Arrows indicate the non-detectable hearing level by profound hearing loss.

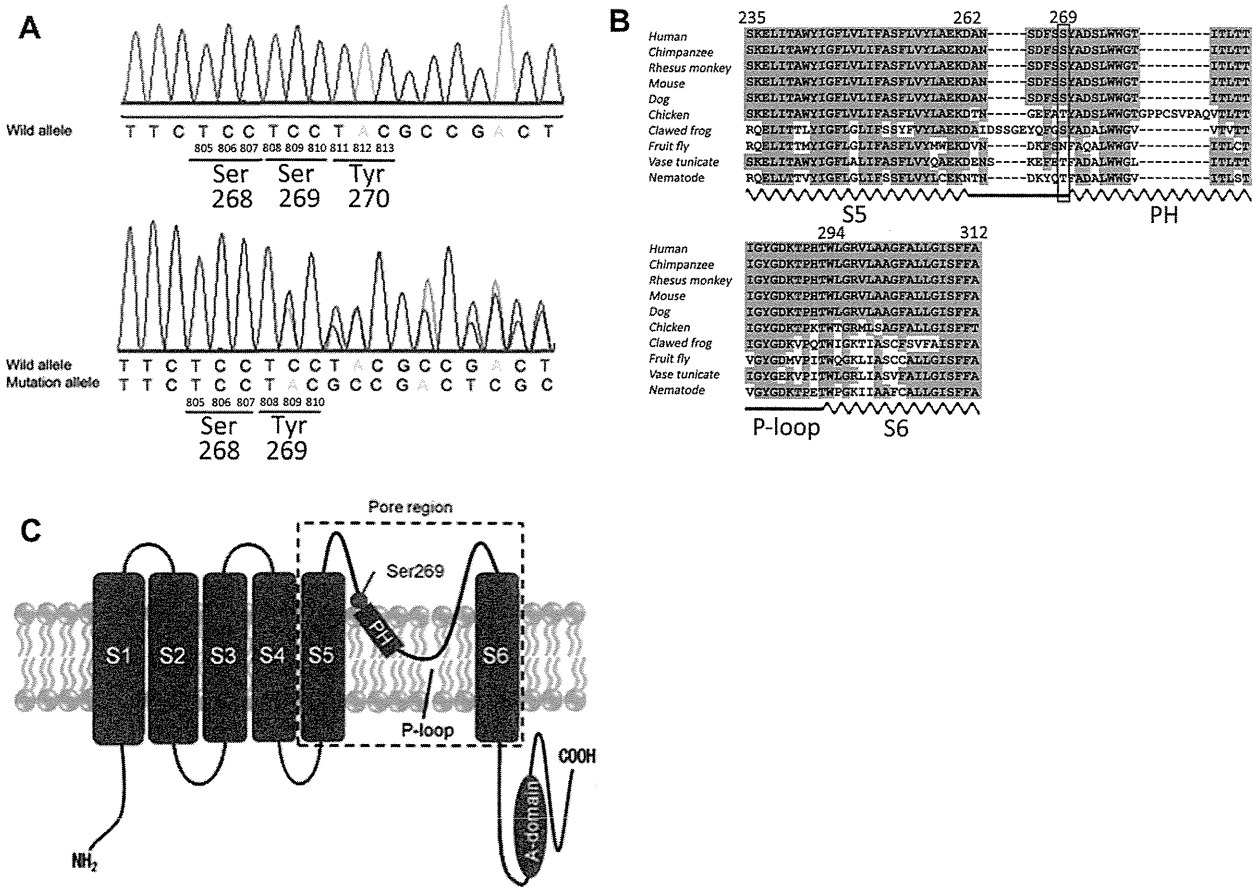

Fig. 2. Partial electrophoretogram of exon 5 of *KCNQ4* with the partial protein sequence for *KCNQ4*. (A) A partial electrophoretogram of exon 5 of *KCNQ4* from an individual with normal hearing (above) and the proband with the heterozygous c.806–808delCCT mutation (below). The positions of the heterozygotic deletion of CCT at 806–808 and the resulting amino acid deletion (p.Ser269del) are indicated. (B) Sequences of the orthologous *KCNQ4* pore region are aligned. Positions highlighted in gray indicate the residues identical to human *KCNQ4*. The position of Ser269 is enclosed by a red square. The positions of S5, pore helix (PH), S6 (wavy lines) and the P-loop (straight line) are shown below the sequences. (C) Schematic topology of *KCNQ4*. Putative domains, including transmembrane regions (S1-S6), channel pore region, PH, P-loop, and A-domain are indicated. Position of Ser269 is indicated by a red circle. (For interpretation of the references to color in this figure legend, the reader is referred to the web version of this article.)

in the region between the putative S5 and PH, a highly conserved region among animal species (Fig. 2B and C). This mutation was found neither on the Exome Variant Server [23] nor in the control group of 96 unrelated Japanese individuals with normal hearing.